Available online at www.sciencedirect.com
ScienceDirect
International Journal of Pharmaceutics 352 (2008) 273–279
INTERNATIONAL JOURNAL OF PHARMACEUTICS
www.elsevier.com/locate/ijpharm

Pharmaceutical Nanotechnology

Injectable actarit-loaded solid lipid nanoparticles as passive targeting therapeutic agents for rheumatoid arthritis

Jiesheng Ye [a], Qun Wang [b], Xuefeng Zhou [a], Na Zhang [a,*]

[a] *The School of Pharmaceutical Science, Shandong University, 44 Wenhua Xi Road, Ji'nan, Shandong Province, China*
[b] *Department of Chemical & Petroleum Engineering, University of Kansas, USA*

Received 18 November 2006; received in revised form 18 September 2007; accepted 17 October 2007
Available online 22 October 2007

Abstract

This work systematically studied the intravenous injection formulation of solid lipid nanoparticles (SLNs) loaded with actarit, a poor water soluble anti-rheumatic drug. The goal of this study was to design passive targeting nanoparticles which could improve therapeutic efficacy and reduce side-effects such as nephrotoxicity and gastrointestinal disorders commonly associated with oral formulations of actarit. Based on the optimized results of single-factor and orthogonal design, actarit-loaded SLNs were prepared by a modified solvent diffusion–evaporation method. The formulated SLNs were found to be relatively uniform in size (241 ± 23 nm) with a negative zeta potential (-17.14 ± 1.6 mV). The average drug entrapment efficiency and loading were (50.87 ± 0.25)% and (8.48 ± 0.14)%, respectively. The actarit-loaded SLNs exhibited a longer mean retention time in vivo ($t_{1/2(\beta)}$, 9.373 h; MRT, 13.53 h) compared with the actarit 50% propylene glycol solution ($t_{1/2(ke)}$, 0.917 h; MRT, 1.323 h) after intravenous injection to New Zealand rabbits. The area under curve of plasma concentration–time (AUC) of actarit-loaded SLNs was 1.88 times greater than that of the actarit in 50% propylene glycol solution. The overall targeting efficiency (TE^C) of the actarit-loaded SLNs was enhanced from 6.31% to 16.29% in spleen while the renal distribution of actarit was significantly reduced as compared to that of the actarit solution after intravenous administration to mice. These results indicated that injectable actarit-loaded solid lipid nanoparticles were promising passive targeting therapeutic agents for rheumatoid arthritis.

Keywords: Passive target; Solid lipid nanoparticles; Actarit; Rheumatoid arthritis

1. Introduction

Rheumatoid arthritis (RA) is characterized by a chronic inflammation of the joint synovium. The precise pathophysiologic cause of RA remains uncertain, however, inflammation is linked to the body's immune system attacking the tissues that line the joints. Medications such as non-steroidal inflammatory drugs can help the patient to feel better but they cannot prevent the damage process itself. Clinical trials using monoclonal antibody therapy are promising (Kavanaugh et al., 1997), but these treatments are expensive and may cause some side-effects such as infection, congestive heart, and malignancy (Keystone, 2005). It is critical to develop an effective vector that can target drugs directly to the immune organ or cells in vivo.

Nanoparticulate systems targeted to macrophages have been proved to be a powerful approach for the treatment of autoimmune blood disorders, diabetes, as well as rheumatoid arthritis (Chellat et al., 2005; Moghimi et al., 2005; Barrera et al., 2000). Following intravenous injection, nanoparticles have a natural tendency to accumulate in the organs that comprise the reticuloendothelial system (RES) (e.g. spleen and liver) (Moghimi et al., 2001). This natural passive targeting tendency could be utilized as a strategy for RA therapy since the targets for RA therapy are the same cells (macrophages) that are responsible for removing the particulates from the blood.

The spleen is the largest immune organ which produces macrophages that are involved in the inflammatory response. An enlarged spleen has been identified as a pathological consequence of RA, especially in patients with Felty's syndrome. Targeting the spleen using the passive targeting tendency mediated by macrophages may improve the therapeutic efficacy and reduce side-effects of disease-modifying anti-rheumatic drugs (DMARDs).

* Corresponding author. Tel.: +86 531 88382015; fax: +86 531 88382548.
E-mail address: zhangnancy9@sdu.edu.cn (N. Zhang).

0378-5173/$ – see front matter © 2007 Elsevier B.V. All rights reserved.
doi:10.1016/j.ijpharm.2007.10.014

Actarit is an orally active DMARDs frequently used in the treatment of rheumatoid arthritis. It has been documented that actarit has a suppressive effect on the progression of articular lesions in mice (Yoshida et al., 1987). Actarit also restored the weight of the spleen to normal, and improved the plasma albumin/globulin ratio of adjuvant arthritic rats (Fujisawa et al., 1990; Fujisawa et al., 1994). However, after oral administration of actarit, much higher concentrations were present in the kidney and gastrointestinal tract than in the plasma; whereas the concentrations in the spleen were lower (Sugihara et al., 1990). Moreover, similar to other DMARDs, most of the major adverse effects were reported to be gastrointestinal disorders after oral administration of actarit (Matsubara, 1999). The urinary abnormalities and renal dysfunction in RA are thought to be induced by DMARDs (Hirofumi et al., 2002). A promising strategy of improving therapeutic efficacy is to enhance the overall targeting efficiency (TE^C) of actarit in the spleen via an intravenous injection route using nanoparticles as drug carriers.

In the present work, we reported the encapsulation of actarit using solid lipid nanoparticles (SLNs) as the drug carrier. SLNs as colloidal drug carriers possess the both advantages of polymeric nanoparticles and liposomes while avoiding some disadvantages such as acute and chronic toxicity in polymeric nanoparticles and overcoming the stability problem in liposomes (Müller et al., 2000). The lipid matrix in SLN is made from physiologically tolerated lipid components, which reduces the potential acute and chronic toxicity.

The aim of this study was to evaluate the efficiency that solid lipid nanoparticles can target actarit to the spleen. In addition, this study aimed to achieve controlled release of actarit while eliminating the adverse side-effects including nephrotoxicity and gastrointestinal disorders typically caused by the oral administration of this drug.

2. Materials and methods

2.1. Materials

Stearic acid was provided by Shanghai Chemical Reagent Co. Ltd. (China). Soya lecithin for injection was obtained from Shanghai Pujiang Phospholipids Co. Ltd. (China). Poloxamer 188 was purchased from Sigma (USA). Actarit was a gift kindly provided by the Research and Development Center of New Drugs in Shandong University (Jinan, China). All other chemicals were of analytical reagent or higher grade.

2.2. Preparation of SLNs

The actarit-loaded SLNs were prepared according to a modified solvent diffusion–evaporation method (de Vringer and de Ronde, 1995; Roberta et al., 1996). In brief, actarit, stearic acid and soya lecithin were dissolved in acetone at 60 °C. An aqueous phase was prepared by dissolving poloxamer188 in doubly-distilled water and heated to the same temperature of the oil phase. The oil phase was dropped into the hot aqueous phase under rapid stirring at 2000 rpm (ETS-D4 stirrer, IKA, Germany) at 60 °C for dispersion. Then the homogeneous suspension was poured into cold water under stirring at 1000 rpm (RW 20.n, Kika Labortechnik, Germany) for 4 h at 2 °C in an ice bath to allow for the hardening of the SLNs. The actarit-loaded SLNs were recovered by centrifugation (Shanghai Anting Scientific Instrument Ltd., China) at 17 000 rpm for 1 h at 4 °C and washed twice using distilled water then re-suspended in 5.0% mannitol (w/v) (lipid content 1.0%, w/v). The resulting suspension were filtered through a membrane with 0.45 μm pore size (Phenomenex, 25 mm filter, CA, USA) and lyophilized (LGJ0.5, Beijing Four-Ring Scientific Instrument Co., China).

2.3. Characterization of SLNs

The morphology of actarit-loaded SLNs was examined using a transmission electron microscope (JEM-1200EX, Jeol, Japan). Lyophilized actarit-loaded SLNs were suspended in doubly-distilled water and filtered through a membrane with 0.45 μm pore size. Samples were prepared by placing a drop of actarit-loaded SLNs re-suspension onto a copper grid and air-dried. Negative staining was conducted with one drop of 3% aqueous solution of sodium phosphotungstate for contrast enhancement. The air-dried samples were then directly examined under the transmission electron microscope.

Size and zeta potentials of actarit-loaded SLNs suspension were analyzed in triplicates by photon correlation spectroscopy and laser Doppler anemometry, respectively, using a particle sizer (Zetasizer 3000 HAS, Malvern Instruments Ltd., Malvern, Worcestershire, UK).

2.4. Determination of entrapment efficiency and drug loading

To determine drug entrapment efficiency and loading, the freeze dried SLNs were dissolved in methanol under water bath at 65 °C for 30 min and then cooled to room temperature to preferentially precipitate the lipid. Drug content in the supernatant after centrifugation (4000 rpm for 15 min) was measured at 246 nm by HPLC using a SPD-10Avp Shimadzu pump and a LC-10Avp Shimadzu UV-VIS detector. Samples were chromatographed on a 150 mm × 4.0 mm^2 reverse phase stainless steel column packed with 5 μm particles (Hypersil ODS, Thermo Electron Corp., Waltham, MA, USA) eluted with a mobile phase consisting of 20:80 mixture of methanol and 2% acetic acid at a flow rate of 1 ml/min (Li et al., 2002). The drug entrapment efficiencies and loading are calculated from Eqs. (1) to (2), respectively.

$$\text{Drug entrapment efficiency (\%)} = \frac{\text{analyzed weight of drug in SLNs}}{\text{theoretical weight of drug loaded in system}} \times 100 \quad (1)$$

$$\text{Drug loading (\%)} = \frac{\text{analyzed weight of drug in SLNs}}{\text{analyzed weight of SLNs}} \times 100 \quad (2)$$

2.5. In vitro drug release

The release of actarit from the SLNs was examined under sink conditions. Five milligrams of actarit-loaded SLNs (equivalent to 0.424 mg actarit) were suspended in 2.5 ml doubly-distilled water and the resulting dispersion or 2.5 ml actarit solution (0.17 mg/ml in 50% propylene glycol, equivalent to 0.425 mg actarit) were put into two dialysis bags (MWCO 12 000, Sigma), respectively. The dialysis bags were subsequently placed in two flasks containing 25 ml dissolution medium (pH 7.4 phosphate buffer containing 0.5% Tween-80) respectively and stirred at 100 rpm in a 37 °C water bath. Aliquots of the dissolution medium were withdrawn at each time interval and the same volume of fresh dissolution medium was added to the flask to maintain a constant volume (Huo et al., 2005). Drug concentrations in the dissolution medium were determined using the HPLC method described in Section 2.4. All experiments were carried out in triplicates. Results are expressed as means ± standard deviation.

2.6. Pharmacokinetics studies in rabbits

The in vivo pharmacokinetics was carried out with adult white New Zealand rabbits weighed 2.0–2.5 kg supplied by the Medical Animal Test Center of Shandong University. All animal experiments complied with the requirements of the National Act on the use of experimental animals (People's Republic of China). The rabbits used for this study were housed individually under normal conditions, and fasted overnight before experiment with free access to water. Animals were randomly assigned to two groups with three rabbits each. Rabbits in one group were administered with actarit-loaded SLNs (equal to 10 mg/kg actarit, 235–300 mg lyophilized actarit-loaded SLNs were suspended in 5 ml injectable normal saline and filtered through a 0.45 μm pore size Phenomenex filter) through one of the ear marginal vein, while control group was administered with 10 mg/kg actarit solution (20–25 mg actarit in 5 ml injectable 50% propylene glycol and filtered through a 0.45 μm pore size Phenomenex filter). One and a half millilitres of blood was withdrawn at specified time intervals (5, 15, 30 min, 1, 1.5, 2.5, 4, 6, 8, 12 and 24 h) from the other ear marginal vein. Plasma samples were harvested by centrifugation at 4000 rpm for 5 min and stored at −20 °C until analysis. Liquid–liquid double extraction was performed prior to analysis by HPLC. Briefly, 500 μl of rabbit plasma was added to 2 ml of hydrochloric acid (0.1 mol/l), and the mixture was extracted with 2.5 ml of dichloromethane vortexing for 120 s. Upon centrifugation at 3000 rpm for 20 min, the organic layer was transferred to another clean test tube and extracted again with 2 ml diethyl ether on a vortex mixer for 120 s. One millilitre of the resulting organic layer was evaporated under nitrogen at 50 °C. The residue was reconstituted with 500 μl of mobile phase and was mixed in a vortex mixer for 90 s (Li et al., 2002). All samples were filtered through a 0.45 μm pore size Phenomenex filter before HPLC determination. The actarit concentration in the plasma was determined using the same HPLC method described above. Pharmacokinetic parameters were evaluated using practical pharmacokinetic program version 97 (supplied by Chinese Pharmacological Society).

2.7. Drug distribution studies in mice

Kunming strain mice, weighed between 18 and 22 g, female or male were provided by the Medical Animal Test Center of Shandong University. Two groups of 18 mice each were used for the in vivo distribution studies of actarit-loaded SLNs or actarit 50% propylene glycol solution. One group was administered with actarit-loaded SLNs (equal to 10 mg/kg actarit) and the other group with actarit solution as control. The mice were anesthetized by inhalation of diethyl ether before blood sample collection. Three mice in each group were taken out randomly at each time interval (15 min, 1, 2.5, 6, 12, 24 h). Blood samples were collected from the ocular artery directly of three mice of each group after eyeball removal and placed into heparinized test tubes. Mice were sacrificed, dissected and each tested organ was removed. Plasma was immediately separated by centrifugation (4000 rpm). Every organ sample was washed with physiological solution and the redundant liquid was blotted using absorbent paper. Accurately weighted tissue specimen was placed in a homogenizing tube with double volume of doubly-distilled water and homogenized in an ice-bath. The extraction of actarit in plasma and the homogenized tissues was operated using the methods described above. Drug concentration in the plasma and homogenized tissues was determined using the same HPLC method mentioned above.

Overall targeting efficiency (TE^C) of actarit-loaded SLNs were calculated and compared with that of actarit solution to evaluate the tissue targeting property of actarit-loaded SLNs. Overall targeting efficiency (TE^C) can be calculated according to Eq. (3) (Wang et al., 2002):

$$TE^C = \frac{(AUC_{0-\infty})_i}{\sum_{i=1}^{n}(AUC_{0-\infty})_i} \times 100\% \quad (3)$$

in which the denominator refers to the sum total of drug exposure to all the tissues, including the target tissue.

The data obtained from pharmacokinetic parameters were analyzed statistically by one-way analysis of variance and *t*-test using a statistical package for social sciences (SPSS version 11.0) software. Statistically significant differences were assumed when $p < 0.05$. All values are expressed as mean ± S.D.

3. Results and discussions

3.1. Formulation optimization and characterization of actarit-loaded SLNs

For all the experiments in the orthogonal design, the encapsulation efficiencies were within a range of 27–50%. Accordingly, we choose the optimized formulation to prepare the blank and actarit-loaded SLNs. The ratio of drug to lipids (w/w), concentration of poloxamer 188 (w/w), time of homogenization (h), and the ratio of soya lecithin to stearic acid (w/w) were chosen as the most influential factors (labeled as A, B, C and D in Table 1). Taking the entrapment efficiency as an index, the four

Table 1
The levels of experimental factors

	A (w/w)	B (w/w)	C (h)	D (w/w)
1	1:5	0.8%	1	1:4
2	1:10	1.6%	2	1:8
3	1:15	2.4%	4	1:15

A, ratio of drug to lipids (w/w); B, concentration of poloxamer188 (w/w); C, time of homogenization (h); D, ratio of soya lecithin to stearic acid (w/w).

Table 2
Orthogonal experiment design and drug entrapment efficiency EE (%) results

	A	B	C	D	EE (%)
1	1	1	1	1	33.29
2	1	2	2	2	36.43
3	1	3	3	3	40.00
4	2	1	2	3	42.43
5	2	2	3	1	31.61
6	2	3	1	2	31.62
7	3	1	3	2	44.31
8	3	2	1	3	49.90
9	3	3	2	1	27.99
K_1	109.72	120.03	114.81	103.71	
K_2	105.66	117.94	106.85	112.36	
K_3	122.20	99.61	115.92	132.33	
K_{11}	36.57	40.01	38.27	34.57	
K_{12}	35.22	39.31	35.62	37.45	
K_{13}	40.73	33.20	38.64	44.11	
R	5.51	6.81	3.02	9.54	

A, ratio of drug to lipids (w/w); B, concentration of poloxamer 188 (w/w); C, time of homogenization (h); D, ratio of soya lecithin to stearic acid (w/w).

factors were investigated at three different levels. The L9 (3^4) orthogonal design was established as shown in Tables 1 and 2. The range, describing the relationship between index and each factor, was drawn to select the optimum ingredient composition which reflected the degree that various factors affected the index. The ranking of the four factors in this experiment was D > B > A > C, and the individual levels within each factor were ranked as: A: 3 > 1 > 2; B: 1 > 2 > 3; C: 3 > 1 > 2; D: 3 > 2 > 1. The optimized formulation should be $A_3B_1C_3D_3$ according to the analytical results using Orthogonality Experiment Assistant version 3.1 (Sharetop Software Studio).

TEM was conducted to investigate the morphology of SLNs. It can be seen that the nanoparticles had spherical or ellipsoidal shapes (Fig. 1). No drug crystal was visible in TEM, and the size as determined from TEM correlated well with the results from the particle sizer (Table 3). The incorporation of actarit into SLNs only resulted in a slight change of average size. Both SLNs presented a negative surface charge that would enhance

Table 3
Average particle size, polydispersity index and zeta potential of blank SLNs and actarit-loaded SLNs (mean ± S.D., $n = 3$)

	Average particles size (nm)	Polydispersity index	Zeta potential (mV)
Blank SLNs	225 ± 18	0.115 ± 0.04	−16.43 ± 5.4
Actarit-loaded SLNs	241 ± 23	0.233 ± 0.11	−17.14 ± 1.6

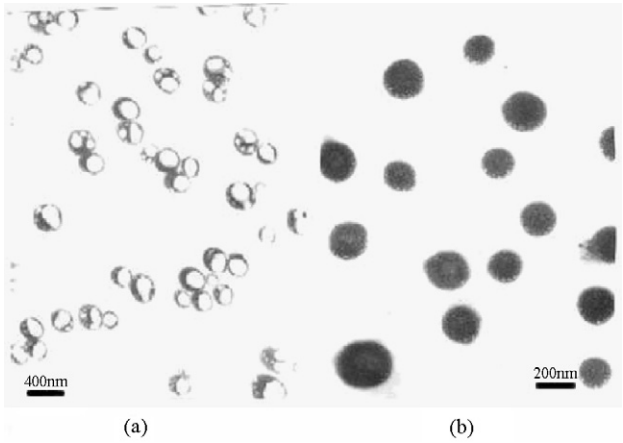

Fig. 1. Transmission electron micrographs of blank SLNs(a) and actarit-loaded SLNs(b).

the colloidal stability of the nanoparticles which have already been stabilized by poloxamer. The incorporation of drug had little effect on the zeta potential.

3.2. Entrapment efficiency and drug loading results

Actarit exhibits a major peak well-separated at 7 min under the HPLC conditions used. The HPLC assay is sensitive enough to detect 0.01 μg/ml of actarit and is linear in the range of 0.01–20 μg/ml ($r = 0.9999$). The orthogonal design experiments indicate that the ratio of soya lecithin to stearic acid (w/w) and the concentration of poloxamer 188 (w/w) are the two most important factors affecting the drug entrapment efficiency. An average entrapment efficiency of (50.87 ± 0.245)% and an average drug loading of (8.48 ± 0.138)% were achieved in the actarit-loaded SLNs with the optimized formulation.

3.3. In vitro drug release

In this study, dynamic dialysis was employed for the separation of free actarit from actarit-loaded SLNs. The solubility of actarit in water was very poor, only 0.104 mg/ml actarit dissolved in phosphate buffer (pH 7.4). In comparison, the solubility of actarit in pure propylene glycol is 5.18 mg/ml. The solubility of actarit at 37 °C could be enhanced to 4.90 mg/ml when 0.5% Tween-80 was added to the phosphate buffer. Therefore, 0.5% Tween-80 was introduced into the drug release medium. Fig. 2 shows actarit release profile from SLNs in phosphate buffer (pH 7.4) with 0.5% Tween-80 at 37 °C.

The release of actarit from actarit-loaded SLNs followed the Ritger–Peppas equation and could be modeled by the following equation: $\ln R = 0.4653 \ln t + 2.4262$, $r = 0.9506$. The release of actarit from actarit solution were fitted to a first order dynamic model and could be expressed by the following equation: $\ln(100\text{-}R) = -0.3256\, t + 4.7256$, $r = 0.9933$. The release profile of actarit from SLNs was biphasic. The initial fast release of around 40% of the drug from the SLNs was observed in the first 8 h, which could be explained by drug desorption from the outer surface of the nanoparticles. Subsequently, actarit-loaded SLNs

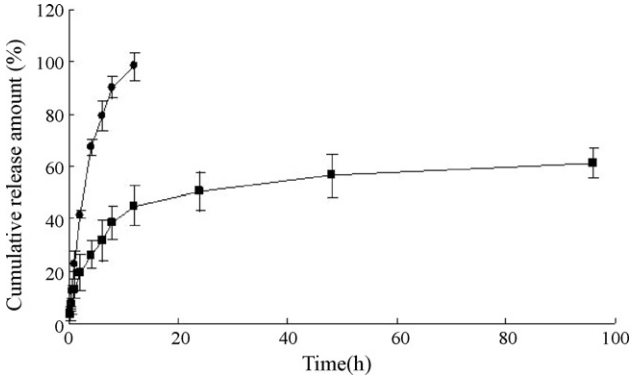

Fig. 2. In vitro release profile of actarit from actarit solution (-●-) and actarit-loaded SLNs(-■-) in 0.5% Tween 80 at 37 °C (mean ± S.D., $n = 4$).

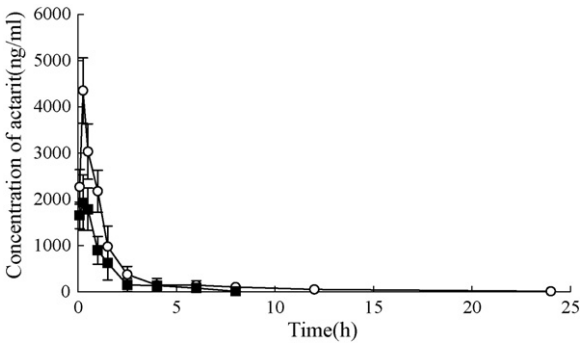

Fig. 3. Mean plasma concentration of actarit after intravenous administration of actarit solution (-□-) and actarit-loaded SLNs(-◯-) (mean ± S.D., $n = 3$).

exhibited sustained–release property and the accumulated drug release percentage at 96 h was only 61.3%. The slow release of the drug in the latter stage was attributed to the fact that the solublized or dispersed actarit can only be released slowly from the lipid matrices through dissolution and diffusion (Grassi et al., 2003). Similar drug release profiles have been reported for SLNs by other groups (zur Muhlen et al., 1998; Liu et al., 2005). In contrast, the release of actarit from the actarit solution is much faster, with near 100% of drug dissolving in the release medium within 12 h.

3.4. Pharmacokinetic studies in rabbits

The chromatograms of actarit showed a stable baseline and good resolution between actarit and endogenous material in plasma. The limit of detection was found to be 5 ng/ml in the present conditions. The assay was linear in the range of 0.01–20 μg/ml. The regression equation was $A = 9332.2C + 26761$ ($r = 0.9983$). The mean absolute recovery of actarit in rabbit plasma was (85.27 ± 3.63)%, and the mean relative recovery was (102.6 ± 5.1)%. Intra- and inter-day accuracy were within the acceptance range of 90–110%. Intra- and inter-day precision were <3%, which were within the acceptance range.

In vivo pharmacokinetic studies indicated that the actarit solution followed a one-compartment model with a rapid terminal elimination phase, while actarit-loaded SLNs followed a two-compartment model with different pharmacokinetic parameters (Table 4). Fig. 3 shows the plasma actarit concentration profiles after administration of SLNs or solution at an equivalent dose.

Table 4
The pharmacokinetic parameters of actarit after i.v. injection of actarit solution and actarit-loaded SLNs to rabbits (mean ± S.D., $n = 3$)

Parameter	Actarit solution	Actarit-loaded SLNs
AUC (ng h/ml)	2980 ± 935	5588 ± 1290*
$t_{1/2(\alpha)}$ (h)	–	0.846 ± 0.135
$t_{1/2ke(\beta)}$ (h)	0.917 ± 0.116	9.373 ± 2.832***
MRT (h)	1.323 ± 0.057	13.53 ± 1.264**
CL_s (mg/h/(μg/ml))	8.389 ± 1.985	4.473 ± 1.365**
V_c (L)	11.103 ± 1.236	7.079 ± 1.296*

* $p < 0.05$ compared with control group.
** $p < 0.01$ compared with control group.
*** $p < 0.001$ compared with control group.

The area under the curve (AUC) determines the bioavailability of the drug for the given dose in the formulation. The AUC (24 h) after i.v. injection was, 2980 ng h/ml for actarit in the solution formulation. The AUC for the SLNs formulation was 5588 ng h/ml, which was 1.88 times greater than the actarit solution formulation ($p < 0.05$). The higher blood concentration of actarit after i.v. injection of actarit-loaded SLNs might be due to the small size of nanoparticles and the coating of poloxamer 188 on the surface of SLNs to keep the particles in the circulation and organ for an extended period of time (Liu et al., 2005).

Another important parameter is the mean residence time (MRT). A prolonged drug residence was achieved. The MRT of actarit-loaded SLNs increased about 10 times compared with the same dose of actarit solution ($p < 0.001$). The extended circulation time might be attributed to the presence of poloxamer 188 on the surface of SLNs and the sustained release of actarit from SLNs. This result was in accordance with previous studies that also demonstrated the potential of using a poloxamer coating to prolong drug circulation time (Illum et al., 1987; Goppert and Müller, 2003; Hu et al., 2005). Similar results have been reported for palmitoyl rhizoxin lipid emulsion and camptothecin solid lipid nanoparticles (Kurihara et al., 1996; Yang et al., 1999).

3.5. Drug biodistribution in mice

The limit of detection was found to be 5 ng/ml and the linearity of the method was demonstrated over the concentration range 0.01–20 μg/ml by analyzing plasma and various tissues standards in triplicate ($r \geq 0.9939$, calibration equations not shown). The absolute recoveries of actarit in mice plasma and tissues were 82.35–91.31%, and the relative recovery was 94.60–106.77%. Intra- and inter-day accuracy were within the acceptance range of 90–110%. Intra- and inter-day precision were <5%, which were within the acceptance range. The actarit concentrations in the spleen and liver of mice after i.v. injection of actarit-loaded SLNs increased from 2.145 and 3.265 μg/g to 5.055 and 6.400 μg/g (15 min), an enhancement of more than 1.96-fold and 2.35-fold, respectively, compared with the same dose of actarit solution ($p < 0.01$; $p < 0.05$) (Table 5).

Table 5
Targeting disposition of actarit after i.v. administration of actarit solution and actarit-loaded SLNs to mice (mean ± S.D., $n = 3$)

Tissue	Actarit-loaded SLNs		Actarit solution	
	C_{max} (μg/g)	AUC (μg/g h)	C_{max} (μg/g)	AUC (μg/g h)
Kidney	11.623 ± 0.115**	12.292 ± 1.325*	14.795 ± 1.896	18.499 ± 2.968
Lung	12.371 ± 0.568*	10.521 ± 2.396	14.461 ± 1.125	11.240 ± 2.354
Spleen	5.055 ± 0.631**	7.345 ± 1.224*	2.145 ± 0.168	2.817 ± 1.299
Liver	6.400 ± 1.288*	5.639 ± 1.001*	3.265 ± 1.097	2.777 ± 0.334
Plasma[a]	12.320 ± 2.998	9.295 ± 3.256	13.567 ± 4.211	7.599 ± 2.735

* $p < 0.05$ compared with control group.
** $p < 0.01$ compared with control group.
[a] Unit of blood drug concentration: μg/ml.

The higher concentrations of actarit in spleen and liver indicated that SLNs mainly accumulated in RES organs (Fig. 4).

These results were in accordance with previous reports on camptothecin SLNs (Yang et al., 1999) and clozapine SLNs (Manjunath and Venkateswarlu, 2005), that demonstrated the passive targeting properties of SLNs towards RES organs.

The actarit-loaded SLNs showed a good spleen targeting property. The spleen TE^C of actarit-loaded SLNs was increased from 6.31% to 16.29% ($p < 0.01$). In contrast, the kidney TE^C decreased from 41.45% to 27.26% ($p < 0.01$) compared with actarit solution (Fig. 5).

These results indicated that actarit-loaded SLNs could successfully target the spleen and correspondingly improve the efficacy of actarit to treat rheumatoid arthritis. The size of particles plays a critical role in their uptake by the splenic sinusoid of animals. Particles greater than 200 nm may act as splenotropic agents (Moghimi et al., 2001; Moghimi, 1995).

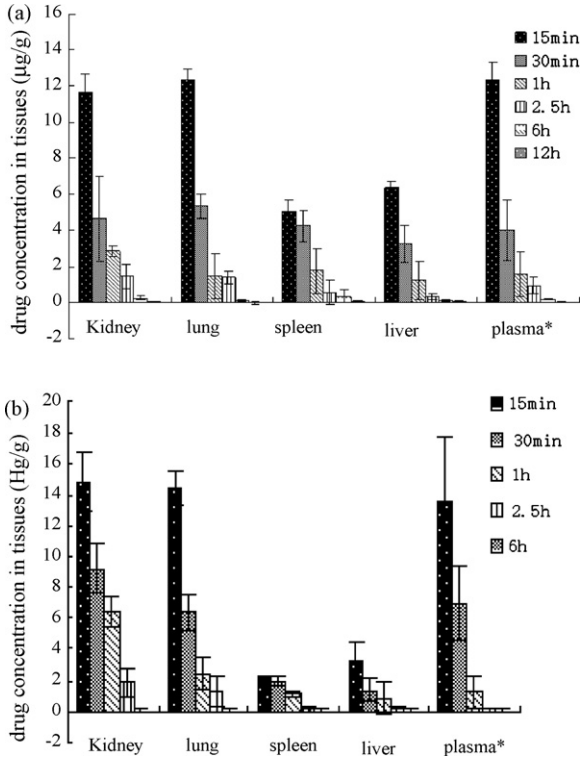

Fig. 4. The distribution of actarit in mouse organs at different time points after i.v. administration of actarit-loaded SLNs (a) and actarit solution (b). *Unit of blood drug level: μg/ml.

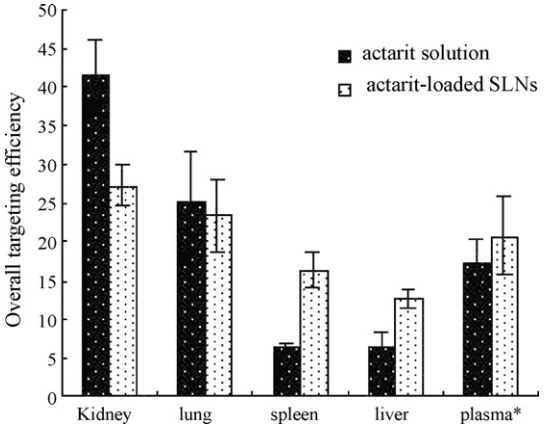

Fig. 5. Overall targeting efficiency (TE^C) of actarit-loaded SLNs and actarit solution (mean ± S.D., $n = 3$).

Actarit is useful for mild to moderate RA and considered reasonable to be used as a first-choice drug in appropriate RA patients (Nagaoka et al., 2002). However, it is difficult to avoid its side-effects such as nephrotoxicity. Actarit is excreted via urine and the kidney is the main elimination organ (Sugihara et al., 1990). The most noteworthy findings of this study were to improve the targeting of actarit-loaded SLNs towards spleen and therefore reduce the accumulation in kidney. The decreased renal accumulation was expected to decrease the risk of nephrotoxicity.

4. Conclusion

In this study, we successfully incorporated the lipophilic anti-RA drug, actarit, into solid lipid nanoparticles. In vitro release tests showed actarit-loaded SLNs exhibited sustained release after an initial burst release. Compared with actarit solution, actarit-loaded SLNs exhibited a prolonged residence time of the drug in the rabbits, and significantly improved the overall targeting efficiency to the spleen of mice. Furthermore, actarit-loaded SLNs can reduce the C_{max} and TE^C in the kidney, potentially decreasing the risk of nephrotoxicity. These results suggest that injectable SLNs may serve as passive targeting agents in RA and may offer reduced doses, decreasing dosing frequency and lowered toxicity, thereby improving patient compliance.

Acknowledgements

We thank Dr. Cory Berkland (Pharmaceutical Chemistry, University of Kansas) for a critical reading of the manuscript. We thank Dr. Min Huang (Pharmaceutical Chemistry, University of Kansas) for helpful discussions. We also thank Tao Wu (Shandong University) for the average diameter, polydispersity index and zeta potential measurements and Ms. Du (Shandong Province Medical Institute) for the transmission electron micrographs.

References

Barrera, P., Bloom, A., van Lent, P.L., van Bloois, L., Beijnen, J.H., van Rooijen, N., de Waal Malefijit, M.C., van de Putte, L.B., Storm, G., van den Berg, W.B., 2000. Synovial macrophage depletion with clodronate-containing liposomes in rheumatoid arthritis. Arthritis Rheumat. 43, 1951–1959.

Chellat, F., Merhi, Y., Moreau, A., Yahia, L., 2005. Therapeutic potential of nanoparticulate systems for macrophage targeting. Biomaterials 26, 7260–7275.

de Vringer, T., de Ronde, H.A., 1995. Preparation and structure of a water-in-oil cream containing lipid nanoparticles. J. Pharm. Sci. 84, 466–472.

Fujisawa, H., Nishimura, T., Inoue, Y., Ogaya, S., Shibata, Y., Nakagawa, Y., Sato, S., Kimura, K., 1990. Antiinflammatory properties of the new antirheumatic agent, 4-acetylaminophenylacetic acid. Arzneimittel-Forsch 40, 693–697.

Fujisawa, H., Nishimura, T., Motonaga, A., Inoue, Y., Inoue, K., Suzuka, H., Yoshifusa, H., Kimura, K., Muramatsu, M., 1994. Effect of actarit on type II collagen-induced arthritis in mice. Arzneimittel-Forsch 44, 64–68.

Goppert, T.M., Müller, R.H., 2003. Plasma protein adsorption of Tween 80- and poloxamer 188-stabilized solid lipid nanoparticles. J. Drug Target. 11, 225–231.

Grassi, M., Voinovich, D., Franceschinis, E., Perissutti, B., Filipovic-Grcic, J., 2003. Theoretical and experimental study on theophylline release from stearic acid cylindrical delivery systems. J. Control. Release 92, 275–289.

Hirofumi, M., Yasuhiko, Y., Yasushi, Y., Yoshitaka, M., Hiroo, H., Masahiro, Y., 2002. Renal involvement in rheumatoid arthritis: analysis of renal biopsy specimens from 100 patients. Mod. Rheumatol. 12, 148–154.

Hu, L.D., Tang, X., Cui, F.D., 2005. Preparation of solid lipid nanoparticles loaded with all-trans retinoic acid and their evaluation in vitro and in vivo. Yao Xue Xue Bao 40, 71–75.

Huo, D.J., Deng, S.H., Li, L.B., Ji, J.B., 2005. Studies on the poly(lactic-co-glycolic) acid microspheres of cisplatin for lung-targeting. Int. J. Pharm. 289, 63–67.

Illum, L., Davis, S.S., Müller, R.H., Mak, E., West, P., 1987. The organ distribution and circulation time of intravenously injected colloidal carriers sterically stabilized with a block copolymer–poloxamine 908. Life Sci. 40, 367–374.

Kavanaugh, A.F., Schulze-Koops, H., Davis, L.S., Lipsky, P.E., 1997. Repeat treatment of rheumatoid arthritis patients with a murine anti-intercellular adhesion molecule 1 monoclonal antibody. Arthritis Rheum. 40, 849–853.

Keystone, E.C., 2005. Safety of biologic therapies–an update. J. Rheumatol. Suppl. 74, 8–12.

Kurihara, A., Shibayama, Y., Mizota, A., Yasuno, A., Ikeda, M., Sasagawa, K., Kobayashi, T., Hisaoka, M., 1996. Enhanced tumor delivery and antitumor activity of palmitoyl rhizoxin using stable lipid emulsions in mice. Pharm. Res. 13, 305–310.

Li, Y.H., Li, J., Jin, Y., 2002. Pharmacokinetics and relative bioavailability of domestic actarit in healthy volunteers. Chin. J. Clin. Pharmacol. 18, 49–52.

Liu, J., Zhu, J., Du, Z., Qin, B., 2005. Preparation and pharmacokinetic evaluation of TashinoneIIA solid lipid nanoparticles. Drug Dev. Ind. Pharm. 31, 551–556.

Manjunath, K., Venkateswarlu, V., 2005. Pharmacokinetics, tissue distribution and bioavailability of clozapine solid lipid nanoparticles after intravenous and intraduodenal administration. J. Control. Release 107, 215–228.

Matsubara, T., 1999. The basic and clinical use of DMARDs. Rheumatology 22, 81–97.

Moghimi, S.M., 1995. Mechanisms regulating body distribution of nanospheres conditioned with pluronic and tetronic block co-polymers. Adv. Drug Deliv. Rev. 16, 183–186.

Moghimi, S.M., Hunter, A.C., Murray, J.C., 2001. Long-circulating and target-specific nanoparticles: theory to practice. Pharmacol. Rev. 53, 283–318.

Moghimi, S.M., Hunter, A.C., Murray, J.C., 2005. Nanomedicine: current status and future prospects. FASEB J. 19, 311–330.

Müller, R.H., Mäder, K., Gohla, S., 2000. Solid lipid nanoparticles (SLN) for controlled drug delivery-a review of the state of the art. Eur. J. Pharm. Biopharm. 50, 161–177.

Nagaoka, S., Ohno, M., Ishigatsubo, Y., 2002. Usefulness of actarit in elderly rheumatoid arthritis. Mod. Rheumatol. 12, 118–127.

Roberta, C., Emilio, M., Lorenzo, R., 1996. Effects of some experimental factors on the production process of solid lipid nanoparticles. Eur. J. Pharm. Biopharm. 43, 110–115.

Sugihara, K., Morino, A., Nomura, A., Iida, S., Sugiyama, M., 1990. Pharmacokinetics of 4-acetylaminophenylacetic acid. 1st communication: absorption, distribution, metabolism and excretion in mice, rats, dogs and monkeys after single administration of 14C-labeled compound. Arzneimittel-Forsch 40, 800–805.

Wang, J.X., Sun, X., Zhang, Z.R., 2002. Enhanced brain targeting by synthesis of 3,5-dioctanoyl-5-fluoro-2-deoxyuridine and incorporation into solid lipid nanoparticles. Eur. J. Pharm. Biopharm. 54, 285–290.

Yang, S.C., Lu, L.F., Cai, Y., Zhu, J.B., Liang, B.W., Yang, C.Z., 1999. Body distribution in mice of intravenously injected camptothecin solid lipid nanoparticles and targeting effect on brain. J. Control. Release 59, 299–307.

Yoshida, H., Fujisawa, H., Abe, C., Shibata, Y., Sato, S., Shiokawa, Y., 1987. Effect of Ms-932 4-acetylaminophenylacetic acid on articular lesions in MRL/I mice. Int. J. Immunother. 3, 261–264.

zur Muhlen, A., Schwarz, C., Mehnert, W., 1998. Solid lipid nanoparticles (SLN) for controlled drug delivery–drug release and release mechanism. Eur. J. Pharm. Biopharm. 45, 149–155.